Progress in Nuclear Magnetic Resonance Spectroscopy 71 (2013) 59–72

Contents lists available at SciVerse ScienceDirect

Progress in Nuclear Magnetic Resonance Spectroscopy

journal homepage: www.elsevier.com/locate/pnmrs

NMR studies of weak protein–protein interactions

Lu-Yun Lian *

NMR Centre for Structural Biology, Institute of Integrative Biology, University of Liverpool, Liverpool L69 7ZB, UK

Edited by J. Feeney and J.W. Emsley

ARTICLE INFO

Article history:
Received 19 August 2012
Accepted 22 November 2012
Available online 20 December 2012

Keywords:
NMR
Weak
Protein
Interactions
Dissociation constants

ABSTRACT

Contents

1. Introduction

1.1. Weak protein–protein interactions

Interactions between proteins are fundamental to life since proteins rarely act in isolation and very little happens in a cell without one protein making contacts with another. Speed and specificity are two opposing features of biological interactions. Protein–protein interactions are either stable or transient [1]. A stable

Abbreviations: CPMG, Carl–Purcell–Meiboom–Gill; CSP, chemical shift perturbation; ETDA, ethylenediaminetetraacetic acid; HADDOCK, High Ambiguity Driven protein–protein DOCKing; nOe, nuclear Overhauser effect; HSQC, heteronuclear single-quantum coherence; IDIS-NMR, isotope-discriminate NMR; ITC, isothermal titration calorimetry; NOESY, nuclear Overhauser effect spectroscopy; PCS, psuedocontact shift; PRE, paramagnetic relaxation enhancement; RDC, residual dipolar coupling; TROSY, transverse relaxation optimised spectroscopy.

* Tel.: +44 151 795 4458; fax: +44 151 795 4404.
E-mail address: lu-yun.lian@liverpool.ac.uk

0079-6565/$ - see front matter
http://dx.doi.org/10.1016/j.pnmrs.2012.11.002

interaction is when the protein exists only in its complexed form and is, hence, a strong interaction. On the other hand, transient interactions are temporary in nature and require a set of conditions, such as conformational changes, phosphorylation or colocalisation within the cell, to promote the interactions. When in complex with interacting partners, transiently interacting proteins are involved in many cellular processes such as folding, electron transfer, protein modification, cell cycling and signalling.

It is now clear that many protein assemblies are weak and/or transient for biological reasons; complexes need to break and reform with specificity and at appropriate rates as part of their biological function and it is energetically preferable if the affinities of these complexes are relatively low. Transient interactions can be strong or weak; strong transient associations require a trigger to shift the equilibrium to the stable state, such as binding of cofactors, whereas in weak interactions, a dynamic oligomeric equilibrium exists with the interaction being broken and formed continuously. Examples of common biological and cellular processes where weak interactions are desirable include reversible cell–cell contacts, rapid enzymatic turnover, electron transfer, transient assembly/reassembly of large, and multiprotein complexes in which target proteins are modified, regulated or translocated to other cellular compartments [1]. In addition, productive, thermodynamically stable specific protein–protein complexes are often formed through the initial assembly of low-affinity, diffusion-controlled complexes.

Weak interactions are characterised by small protein–protein interfaces. Typically, protein–protein interactions interfaces are over 1500 Å^2; for weak complexes, however, the interface area can be as low as 500 Å^2 [2]. In terms of strengths of interactions, K_D values ($K_D = k_{off}/k_{on}$) less than 10^{-9} M are described as strong interactions, and K_D greater than 10^{-4} M, weak interactions. In protein–protein interactions, k_{on} is approximately 10^5–10^6 M^{-1} s^{-1} [3]; hence, for transient interactions, k_{off} can be as fast as 10^4 s^{-1}. In the cell, a majority of the protein–protein interactions occur with K_D less than 10^{-6} M.

Being able to detect and characterize these weak complexes is crucial for understanding biological processes, mechanisms and pathways. The common biophysical techniques for studying weak protein–protein interactions include hydrodynamic methods, surface plasmon resonance, isothermal titration calorimetry, nuclear magnetic resonance spectroscopy (NMR) and optical techniques such as fluorescence resonance energy transfer and bioluminescence resonance energy transfer [4]. However, NMR spectroscopy, is the most versatile and information-rich for reasons given below.

Central to the function of a protein and its interactions are the dynamics of the protein and, hence, methods such as NMR that are able to detect and characterise these are particularly powerful [5]. In addition, interaction effects are not restricted to the localised, contact interface between two proteins; rather information can be transmitted throughout the molecule [6]. NMR is able to provide such information for the entire protein at atomic detail. It is undoubtedly one of the best techniques for measuring dynamics and conformation changes. The method is suited for interactions associated with the very rapid dissociation rates (k_{off}) that are often found in weak protein–protein complexes [7–14]. The types of information obtainable from NMR studies of weak complexes range from complete structure determination to examinations of low resolution datasets which simply highlight the possible regions involved in intermolecular interactions. Between these extremes, other types of structural and dynamics information can be obtained including providing affinity constants [15], and detecting binding intermediates [16]. To obtain high resolution structures of a complex, NMR-derived restraint-driven docking and energy minimisation methods are used, provided that the structures of the individual components are known [17–20]. For weak interactions, combined NMR and functional studies, often involving mutagenesis, have been shown to be one of the most effective approaches for detecting otherwise undetectable interactions.

One main drawback of the NMR method is the low sensitivity; in very weak interactions the population of molecules in the complexed forms are often very low, posing a significant practical challenge in NMR studies. Two recent approaches have been particularly useful for detecting lowly populated species which may also be transient. These are paramagnetic relaxation enhancements (PREs) [21,22] and relaxation dispersion spectroscopy [23]. Furthermore, because many of the NMR experiments are conducted under equilibrium conditions, it is often possible to increase the population of complexed forms by increasing the initial concentrations of the interacting proteins.

The focus of this review is on the use of NMR to study weak heterotypic protein–protein interactions in which complexes are formed between different proteins rather the homotypic interactions which lead to the multimerisation of a particular protein. Section 2 describes methods for preparing weak protein complexes for NMR studies, and includes the different types of isotope labelling that are required, as well as the practicalities of making protein–protein complexes that are functionally relevant. Sections 3–6 describe the common NMR techniques that can be used to study weak protein–protein complexes; although many of these are similar to those used for the investigation of tight complexes, some are particularly relevant for the weaker complexes. Furthermore, in studies of weak interactions, the different techniques can be used in the 'titration' mode where the NMR characteristics are observed as a function of increasing concentrations of a partner protein, rather than as a single equilibrium mix with only one protein:protein concentration ratio; in this mode special considerations must be given as to how the parameters in the fully bound forms are derived [24,25]. Section 8 describes how NMR-derived information can be integrated with docking software to enable the determination of the structures of protein complexes; this latter hybrid method is proving to be a very powerful approach for the weakly-interacting protein complexes. Many of the techniques and approaches described here can also be found in Ref. [26] and Table 1 summarises examples of the weak complexes which have been studied in some detail.

1.2. NMR timescales

The success of an NMR method is dependent on the compatibility of the particular chosen experiment with the dynamics of the system under consideration. This is particularly pertinent to weak protein interactions where the populations of some of the states of interests are very low.

The term exchange rate between species, k_{ex}, is often used in NMR. It is related to the commonly used term k_{off} or k_{-1}(off rate) for interactions between protein E and ligand L by the equation $k_{ex} = k_{off}/p_L$ (when detecting the ligand signal) and $k_{ex} = k_{off}/p_E$ (when detecting the protein signal) where mole fraction $p_L = [L]/L_T$ (and $L_T = [L] + [EL]$, $[L]$ is the concentration of ligand in the free state) and mole fraction $p_E = [E]/E_T$ (and $E_T = [E] + [EL]$) [26]. The exchange rate is defined on the NMR timescale by considering the lifetimes of each state relative to the difference in the NMR parameters of chemical shift, scalar coupling or relaxation rate. The chemical shift is the most common parameter, although exchange regimes on the relaxation timescales are becoming important especially when using relaxation-based characteristics such as PRE and relaxation dispersion experiments. When using the chemical shift timescale, in a second-order exchange between two molecules A and B as shown in Eq. (1), *slow exchange* is defined by $k_{ex} \ll |\delta_A - \delta_B|$ where δ_A and δ_B are the chemical shifts in Hertz (Hz) in the two states, *intermediate exchange* defined by

Table 1
Examples of Weak Protein–Protein complexes studied by Nuclear Magnetic Resonance.[a]

	K_D[b]	Information[c]	References
Chemical shift perturbations (CSPs) and intermolecular nOes			
Ubiquitin-CIN85 SH3 A	500 μM	NMR determination of K_D; mapping binding surface	[33]
Ubiquitin-CIN85 SH3 B	1150 μM	NMR determination of K_D; mapping binding surface	[33]
Ubiquitin-CIN85 SH3 C	171 μM	HADDOCK model based on CSP, PRE and RDC; Relaxation dispersion experiments	[33,56]
Ubiquitin-CD2AP SH3 C	132 μM	RDC Titration, IDIS-NMR and HADDOCK model	[24,74]
Ubiquitin-SlaI SH3-C	40 μM (25 °C); 400 μM (45 °C)	Intermolecular NOE; structure of complex	[78]
Ubiquitin–Ubiquitin Conjugating enzyme Mms2	98 μM	NMR determination of K_D	[79]
Ubiquitin- Ubiquitin Conjugating enzyme Uev1a	213 μM	NMR determination of K_D	[79]
Ubiquitin-CUE	200 μM	NMR determination of K_D; intermolecular NOE; structure of complex	[80]
PINCH-1 LIM4-Nck2 SH3-3	3 mM	Intermolecular NOE and model of complex	[12,38]
Myosin LC phosphatase-Leucine zipper	178 μM	Chemical shift perturbation and line broadening	[81]
MUC1 cytoplasmic domain-Src-SH3	2–3 mM	Chemical shift perturbations to map interaction surface	[82]
MUN-Munc 18-1	150 μM	NMR determination of K_D through linewidth titration; mapping binding surface	[34]
MUN-Syntaxin-1 SNARE motif	46 μM	NMR determination of K_D through linewidth titration; mapping binding surface	[34]
Anp32 LRR-PP2A	mM	Chemical shifts perturbation	[32]
E. Coli Phosphotransferase System Enzyme II A domain (H554Q)-B domain (C384S)	3700 μM	Chemical shift changes; structure determination using filtered nOes	[39]
GFP (jellyfish) – phosphoprotein clytin	900 μM	Chemical shift changes and HADDOCK structure based on shift changes	[83]
Lipoyl domain – E1component of Pyruvate Dehydrogenase complex of *B. Stearothermophilus*	400 μM	T2 relaxation in combination with chemical shift and site-directed mutagenesis to identify interaction sites	[84]
Pilus intersubunit interactions involving *E. Coli* Type 1 Pilus Subunit FimF	~10000 μM	Chemical shift changes, intermocular nOes, PRE	[85]
Cross-saturation			
B domain of Protein A – Fc fragment of Immunoglobulin G	~0.4 μM	Identification of binding interface and comparison with CSP, deuterium exchange and X-ray structures.	[41]
SH3 domain from p67(phox) - non-PxxP peptide	10 μM	Identification of binding site on Sh3	[86]
SH3 domain from Grb2 - non-PxxP peptide	10–20 μM	Identification of binding site on SH3	[86]
SH3 domain from Pex13p - non-PxxP peptide	1 mM	Identification of binding site on SH3	[86]
Cytochrome b5-cytochrome c	2.5 μM	Identification of binding site on cytochrome c	[87,88]
Transferred cross saturation			
B domain of Protein A – Immunoglobulin G (Mr. 164kD	0.26 μM	Identification of bindng site on A-domain	[43]
Pseudoazurin-nitrite reductase (Mr. 110kD)	64 μM	Mapping interaction surface on pseudoazurin	[68]
Ferredoxin-sulphite reductase (Mr. 65kD)	13 μM	Mapping interaction surface on ferredoxin	[89]
Toxin AgTx2-KcsA K + channel (Mr. 70kD)	400uM	Identification of KcsA-binding interface on AgTx2 in bilayers	[90,91]
Antimicrobial peptide Sapecin – phospholipid vesicle	80 μM	Identification of protected residues, membrane insertion site and membrane permeabilisation mechanism.	[92]
Collagen-DS domain from disciondin domain receptor 2	25 μM	Collagen-binding surface on DS domain	[93]
Paramagnetic effects			
Bacterial phosphotransferase system	5 μM	Presence of transient low population species	[66,70,94]
IsdA:heme:IsdC heme complex	>5 mM	PRE-derived model of complex	[95]
Plastocyanin-cytochrome c	67 μM	Paramagnetic line-broadening; mapping binding interface	[61]
Plastocyanin-Ferric cytochrome f	62.5 μM	Characterisation of complex based on extensive analyses of paramagnetic effects; pseudocontact shifts as structural restraints; model of complex	[67,96]
Pseudoazurin-nitrite reductase	64 μM	PRE-derived model using from Gd3 + -CLanP-1 tagged NR	[97]
Adrenodoxin-cytochrome c	25 μM	Ensemble of structures for cross-linked complex	[98]
Cytochrome b5-cytochrome c	2.5 μM	PRE-derived model of complex	[99]
Residual Dipolar Coupling			
CD2AP SH3-C-ubiquitin	132 μM	RDC-derived model of complex	[24]
Relaxation dispersion			
Abp1pSH3-Ark1p peptide	0.5 μM	Relaxation dispersion to obtained chemical shifts for structural calculations	[58]
CIN85 SH3 C-ubiquitin	171 μM	Intermediates in interaction pathways – three-site binding	[56]

[a] Examples listed are not exclusively for weak complexes; some of the methods used in the studies of tighter complexes are also applicable to weak interactions.
[b] Approximate K_D values, sometimes quoted as a range.
[c] CSP, chemical shift perturbation; PRE, paramagnetic relaxation enhancement; RDC, residual dipolar coupling.

$k_{ex} \sim |\delta_A - \delta_B|$, and *fast exchange* by $k_{ex} \gg |\delta_A - \delta_B|$. For weak interactions, the fast and intermediate exchange regimes are most relevant. When discussing chemical exchange, the chemical shifts are expressed in frequency units (Hz or radian s^{-1}) rather than in the dimensionless ppm. The appearance of the spectrum will, therefore, be dependent of the magnetic field strengths. Hence, spectra at higher field strengths will show slower exchange behaviour; systems undergoing moderately fast exchange at 14.1T (600 MHz) could appear to be in intermediate exchange at 18.79T (800 MHz). Typical chemical shift differences are of the order of a few hundreds of Hertz. To determine the most appropriate NMR experiment or parameters to use, it is, therefore, important at the initial stages of a study to qualitatively establish the chemical exchange regime of the system.

Weak protein interactions are often characterised by high dissociation rate constants, k_{off}, resulting in the averaging of the NMR signals from the free and bound states. Through this exchange mechanism, it is possible to obtain information of the low population bound state by analysing the resonances from the free form in exchange with the bound form; this characteristic is frequently exploited in the different experiments described in this review and is one of the main advantages of the NMR method.

2. Preparation of samples

2.1. Determining dissociation constant and estimating population of bound species for weak complexes

A factor to consider when designing an NMR study of protein–protein complexes is the population of the protein that is in the complexed form. A simple binary, second-order interaction between two proteins is considered here.

$$A + B \underset{k_{-1}}{\overset{k_{+1}}{\rightleftharpoons}} AB \tag{1}$$

where k_{+1} and k_{-1} are the association and dissociation rate constants, respectively. The dissociation constant for the reaction is define d as:

$$K_D = \frac{k_{-1}}{k_{+1}} = \frac{[A][B]}{[AB]} \quad \text{and} \quad \left(K_D = \frac{1}{K_{\text{eq}}} \equiv \frac{1}{K_A}\right) \tag{2}$$

where K_D is the dissociation constant, K_{eq} the equilibrium constant which also equivalent to the association constant, K_A. If the dissociation constant K_D and $[A]$ and $[B]$ are the concentrations of the free proteins, then the concentration of the complex $[AB]$ can be calculated using the equation above.

The mole fraction, $p_{A,\text{bound}}$ of a protein A in complex with B, where B is considered the "ligand" is given by:

$$p_{A,\text{bound}} = \frac{[AB]}{[A]_T} = \frac{1}{2[A]_T}\left\{[A]_T + [B]_T + K_D - \sqrt[2]{(([A]_T + [B]_T + K_D)^2 - 4[A]_T[B]_T)}\right\} \tag{3}$$

when $[A] \geqslant [B]$, such as when undertaking a titration of A by increasing concentrations of B, and total concentrations $[A]_T = [A] + [[AB]$ and $[B]_T = B + [AB]$ [26]. However, when the $[B] \gg [A]$, then the mole fraction of bound A (or the fractional saturation of A) can be simplified to:

$$p_{A,\text{bound}} = \frac{[B]_T}{[B]_T + K_D} \tag{4}$$

In the studies of weak interactions Eq. (4) is useful for estimating the highest possible value of the mole fraction of bound A. For example, if the K_D is 200 μM, and $[A]$ and $[B]$ are each 1 mM, $\rho_{A,\text{bound,max}}$ is 0.83; if $[B]$ is 10 mM, $\rho_{A,\text{bound,max}}$ is 0.98. That is, at a 10-fold excess of ligand B, the bound state can only be populated to 98%. This calculation implies that it is almost impossible to obtain information on the truly bound state. Unlike small ligand titrations, in a protein–protein complex, excessively high concentrations are limited by the solubility or the aggregation tendency of the titrant protein. More often than not, as a compromise between obtaining sufficient signal-to-noise and protein aggregation/solubility, most protein complexes are studied in range of 1:1–1:5 (protein:titrant) and hence, often are not in the fully complexed state (except where the K_D is in the nanomolar range). For weak complexes, therefore, new approaches have been devised for extrapolating the relevant parameters of the bound state, as highlighted in this review.

2.2. Isotope labelling

The success of the isotope-filtered experiments, which are often used to detect intermolecular nuclear Overhauser effects (nOes), rests on having proteins labelled close to 100%. Therefore, it is important, when using minimal media to prepare ^{13}C and ^{15}N proteins that isotopic dilution is minimised by growing pre-cultures in labelled media (rich or minimal) before inoculating the main labelled culture with the labelled starter culture.

The most common labelling strategy for NMR studies of protein–protein complexes is for one component to be isotopically labelled and the other unlabelled. If the aim is to obtain information from both components of a complex, then two samples are often needed, one with the first protein labelled and the second with the other labelled. The main labelling patterns are uniform $^{13}C/^{15}N/^{2}H$, amino acid-specific $^{13}C/^{15}N$, and ^{13}C Ile, Leu, Val, Ala-methyl group [27].

If non-exchangeable protons (those bound to carbon atoms) are not required, then deuteration is advantageous; line-broadening effects due to unfavourable exchange rates and tumbling times, are alleviated, thereby improving sensitivity. These benefits can be seen even with ~80% deuteration, which is the level that is easily achievable using D_2O-based bacterial growth media. In weak protein–protein complexes, it is unlikely that deuteration of the partner protein will be beneficial since the major cause for relaxation is from the nearest, intramolecular protons.

More recently, rather than labelling only one component, differential labelling of both components of a complex at the same time have been reported [28,29]. In the 'isotope-discriminate NMR (IDIS-NMR) approach, one sample is doubly-labelled with ^{13}C, ^{15}N and the other component singly with ^{15}N. 2D $^{1}H,^{15}N$-correlation spectrum is observed for both samples; however, the J-couplings to the ^{13}C nuclei enable the spectrum to be edited for or against the doubly-labelled protein component [29]. Information for both components of the complex can be obtained from just one sample, although this approach is less sensitive that the normal $^{1}H–^{15}N$ heteronuclear single-quantum coherence/ HSQC/TROSY experiments. NMR parameters such as chemical shifts, ^{15}N-relaxation times, residual dipolar couplings for both components of the complex can be measured at the same time using this isotope discrimination method [30]. Although having the advantage of requiring only one sample, hence, reducing cost and sample variability, there are limitations of this approach. For example, for very weak binary complexes it is necessary to use a large excess of one component to achieve saturation. This makes IDIS-NMR unsuitable since the two observable components would be at different degrees of complexation. The IDIS-NMR method fares better for a ternary complex where two proteins interact with a third common component; the latter need not be labelled and can be in excess, allowing the behaviour of the other two labelled components to be studied simultaneously. The CD2AP SH3-C-ubiquitin structure was determined using this approach [24].

2.3. Preparation of the protein–protein complexes for NMR studies

The conventional method is to titrate one protein into another until saturation is reached. In the case of fast chemical exchange, this is conveniently done by tracking the chemical shift changes with increasing additions of the titrant until no further chemical shift changes are observed. This method has the disadvantage that one component in the titration experiment is required to be at high concentration and most proteins aggregate at these concentrations. Hence, a better method is to premix and equilibrate the two proteins in known ratios in dilute concentrations and then concentrate the mixture to the desired concentration using spin sample concentrators or stirred cells, retaining the ratio between component proteins. Separate complex samples for each titration point can be made using the same stock of proteins in order to minimise variations in sample conditions within a set of experiments [31].

3. Chemical shift perturbation

Chemical shift perturbation is the simplest and almost always the first step for detecting interactions between proteins since it

is a very sensitive approach. Perturbations can take the form of changes in chemical shifts or line-broadening effects. For this method to be reliably used, the perturbations must be selective rather than affecting all resonances, especially at substoichiometric amounts of the titrant protein. As the titrant is added to excess, resonances of the bound form will either be observed in a shifted position or severely broadened to the extent that they are unobservable. While universally used to detect binding, the use of chemical shift perturbations for establishing sites of interactions must be used with caution since the shifts changes can be caused by a variety of factors including conformational changes. However, since weak protein–protein interactions are often not accompanied by significant conformational changes (with the exception when flexible regions are involved) the chemical shift perturbation method is ideal for this category of interactions.

The most convenient and sensitive NMR method, with very high information content, for detecting chemical shift perturbations is the ^{15}N–^{1}H HSQC experiment. Almost all the protein–protein complexes studied use this method. In very weak interactions, the shift changes can be very small but yet discernable, as shown in Fig. 1 [32]. A reference spectrum of the free ^{15}N-labelled protein is acquired first followed by a spectrum of the protein in the presence of increasing amounts of the unlabelled interacting partner. In most cases, if there is interaction, the chemical shift of the labelled protein would shift linearly with increasing amounts of the unlabelled protein when the free and complexed proteins are in fast chemical exchange on the NMR timescale, reaching a plateau at saturation; this linear shift is a consequence of the equation for that weighted average which defines the observed chemical shift (if there is only a simple two-state equilibrium between free and bound states) as:

$$\delta_{A,\mathrm{obs}} = \delta_{A,\mathrm{free}}(1 - p_{A,\mathrm{bound}}) + \delta_{A,\mathrm{bound}} p_{A,\mathrm{bound}} \quad (5)$$

where $\delta_{A,\mathrm{obs}}$, $p_{A,\mathrm{bound}}$, $\delta_{A,\mathrm{free}}$ and $\delta_{A,\mathrm{bound}}$ are, respectively, the observed chemical shift, the mole fraction of bound A and the chemical shift of A in the free and complexed form. Fig. 2 shows the typical titration example from an NMR ^{15}N HQSC titration [33]. In these experiments, ubiquitin was separately titrated into solutions

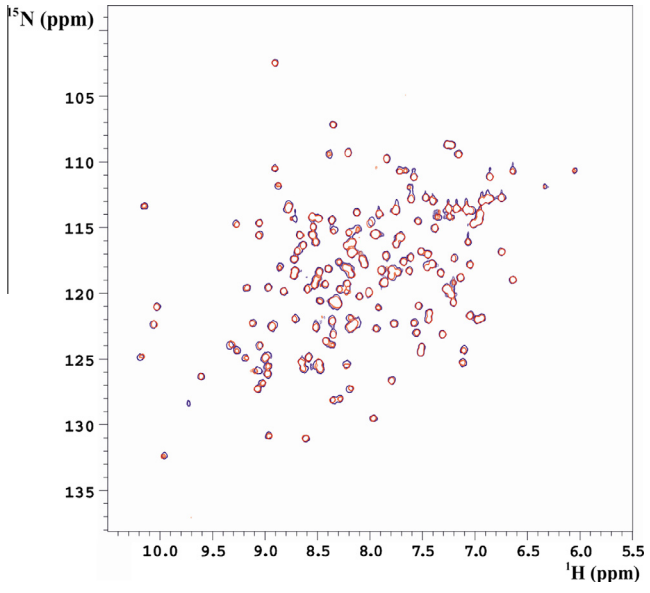

Fig. 1. ^{15}N–^{1}H HSQC spectrum (at 14.1T) of ^{15}N-labelled Anp32a leucine rich repeat (200 μM) in the absence (blue) and presence (red) of a three fold excess of unlabelled Atx1 AXH domain. The weak complex is formed with K_D in the millimolar range. The chemical shift changes, although very small, are discernable and specific to show that binding is present. Reproduced with permission from de Chiara et al. (2008) Febs Journal 275: 2548–2560, John Wiley and Sons.

of three SH3 domains from Cbl ubiquitin-ligase interacting protein, CIN85 (CIN85 SH3-A, -B and -C) and *vice versa*.

Chemical shift perturbations are able to detect interactions over a very wide K_D range. Apart from qualitatively detecting binding and identifying binding sites/interfaces, these perturbations are most commonly used to extract binding affinities of weak interactions where no other methods are available. However, it must be used with caution as the method is not as precise as other biophysical methods because of the stringent requirement that the system must be in truly fast exchange before reliable results can be obtained. Ideally, there should be no significant line-broadening in the shifted resonances during the titration; however, this condition is not often met for all the resonances because the magnitude of chemical shift differences can vary substantially between resonances. As the overall K_D value is obtained by averaging over many resolved resonances this can lead to significant inaccuracies. At best, therefore, the K_D values obtained using NMR titration should be treated as estimates.

In terms of how K_D values can be obtained from an NMR titration, under the very fast exchange regime and for 1:1 complexes, a global, non-linear least squares fit of the following equation is often used:

$$\Delta\delta = \frac{(\delta_{A,\mathrm{bound}} - \delta_{A,\mathrm{free}})}{2[A]_T}\left\{[A]_T + [B]_T + K_D - \sqrt[2]{(([A]_T + [B]_T + K_D)^2 - 4[A]_T[B]_T)}\right\} \quad (6)$$

where $\Delta\delta$ is the chemical shift difference between the observed shift and that of free A ($\delta_{A,\mathrm{bound}} - \delta_{A,\mathrm{free}}$) is the chemical shift difference between fully bound and free A, $[A]_T$ and $[B]_T$ are the total concentrations of proteins A and B, where B is the titrant (ligand) and K_D is the dissociation constant [26]. In weak binding, it is often difficult to reach saturation because of the limitations on protein solubility and behaviour (aggregation at high protein concentrations). As a result K_D is often underestimated. A full discussion on this method for estimating K_D values is given in [15].

In general however, for the majority of protein–protein complexes, it is rare for resonances to experience no line-broadening; instead, a gradual increase in linewidths and decreasing signal to noise ratio is the norm (Fig. 3A). This feature limits the use of chemical shift perturbations to providing only a broad indication of the protein–protein binding interface which can be further confirmed by more precise NMR methods such as cross-saturation or intermolecular nOes or by mutagenesis. If a resonance of the bound form is observed, more detailed experiments such as those described in later sections can be performed. Among the causes of the line-broadening effects are dynamic protein–protein interfaces, increase in the molecular mass of the complex or unfavourable chemical exchange between free and complexed forms. When the signal of the complexed form is not observable even in the presence of large excess of the titrant and after deuterating both the titrant and the titrated, it is difficult to establish the end-point of a titration. Here, a combination of two titrations could be performed, one using the protein partner as the titrant and the other using a peptide fragment from the protein partner. Since the latter complex is, in principle, less prone to detrimental line-broadening effects, it is possible to use the titration of the peptide as a proxy for the protein titration in order to obtain the resonance position of the fully complexed labelled protein; the important feature is that the chemical shift changes in the labelled protein caused by the partner protein and its peptide are collinear and at some point in the protein and peptide titration, these shift resonances overlap. An example of how this approach works is shown in Fig. 3B, for the interactions between the potassium inward rectifier, Kir2.1 (Mr. 128 kD), and the PDZ domain region of SAP97 (Mr. 36 kD); in this study the 10 amino acid at the C-terminus of Kir2.1 which forms the main binding site of Kir2.1 to the PDZ domains was used.

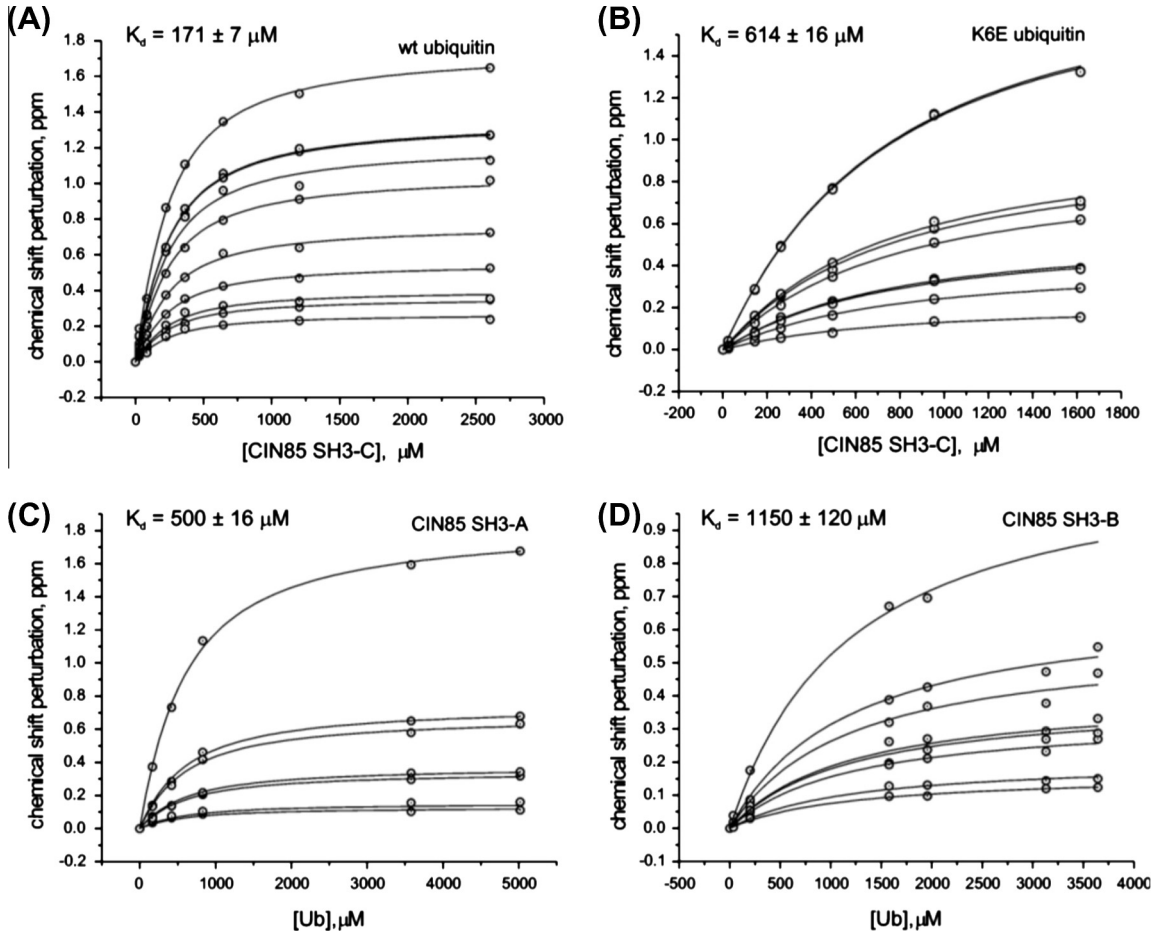

Fig. 2. Binding curves for the interaction between ubiquitin and SH3 domains of the adapter protein CIN85 obtained from chemical shift changes in the ^{15}H–^{1}H HSQC spectra. A global fit of selected number of residues (given in parenthesis) in each experiment is performed using Eq. (6). Chemical perturbation of (A) ^{15}N-labelled wild-type ubiquitin (10 residues) and (B) ^{15}N-labelled mutant ubiquitin (9 residues) titrated with unlabelled CIN85 SH3-C. Chemical perturbation of (C) ^{15}N-labelled CIN85 SH3-A (7 residues) and (D) ^{15}N-labelled CIN85 SH3-B (8 residues) titrated with unlabelled ubiquitin. Reproduced with permission from Bezsonova et al. (2008) Biochemistry 47: 8937–8949, American Chemical Society.

Although many projects are prematurely terminated because of severe line-broadening as the complexes are formed, a careful analysis of this line-broadening effects can be used to assess relative binding affinities as shown in Fig. 3 C and D, or to estimate K_D values [31,34,35].

4. Nuclear overhauser enhancement

4.1. Intermolecular NOE

NOE constraints are by far the main NMR restraints used for the calculations of protein structures. In principle, the approaches used for the calculations of the structure of a single protein can also be used for determining the structure of a protein complex, and when detectable, these NOE restraints are the most important restraints for producing good structures of the complexes. In weak complexes, however, intermolecular nOes may be undetectable due often to intermediate exchange, line broadening or low concentrations as a result of low solubility of the protein complexes. Specific assignments of the intermolecular nOes can also be difficult and requires prior knowledge of the resonance assignments of both partners of the complex.

In almost all cases, the nOes between protomers in a complex are detected using isotope-filtered experiments and there are many versions of this experiment, all using hetero-labelled protein complexes in which only one protomer is labelled at any one time [36]. The most common combination is $^{13}C/^{15}N$ sample of one protein complexed with another unlabelled protein and *vice versa*. It is not necessary to deuterate the other partner. Double half-filtered nuclear Overhauser effect spectroscopy (NOESY) experiments are used to obtain nOes between pairs of protons in which one proton is from the $^{13}C/^{15}N$-labelled protein and the other is from the bound, unlabelled partner. Intermolecular nOes are obtained and unambiguously identified. It is important that the filtered experiments are optimised experiments in order to prevent or reduce 'breakthrough' which could complicate the data analyses.

Two types of half-filtered NOESY experiments are normally used to obtain the intermolecular nOes: ^{13}C-separated-^{15}N,^{13}C-filtered NOESY detects nOes between ^{13}C protons of a ^{13}C,^{15}N-labelled protein and CH and NH proton from the unlabelled protein, and the complementary ^{15}N-separated ^{15}N,^{13}C-filtered NOESY which detects nOes between ^{15}N protons of a ^{13}C,^{15}N-labelled protein and CH and NH proton from the unlabelled protein. These are inherently insensitive experiments. As an alternative, the ^{15}N-edited NOESY on a ^{15}N-deuterated protein bound to an unlabelled protein will detect nOes between the amide protons of the ^{15}N-labelled protein and any protons in the target protein that are in close proximity [37].

A survey of the application of these half-filtered experiments show that they work best in high affinity complexes where

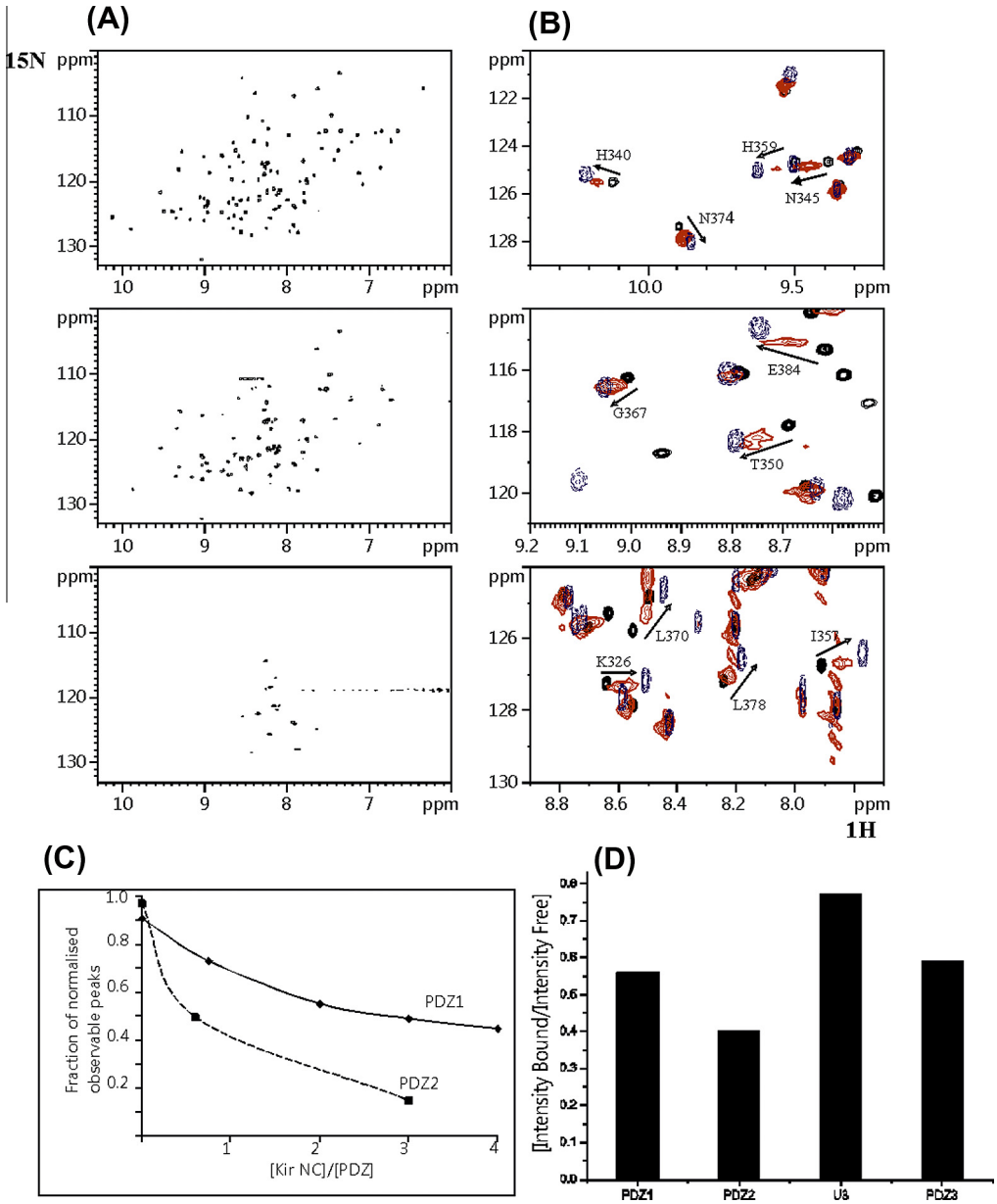

Fig. 3. SAP97 PDZ interactions with KirNC (A) ^{15}N–^{1}H HSQC spectrum (at 14.1T) of ^{15}N-labelled PDZ2 (Mr. 10kD) in the presence of increasing amounts of unlabelled Kir2.1NC (148kD). Concentration ratios of PDZ2 to KirNC are 1:0 (top) and 1:4 (bottom). Many resonances from the PDZ domain are significantly broadened in the presence of excess KirNC. (B) Chemical shift perturbation of selected residues from SAP97 PDZ2 by increasing concentrations Kir2.1NC (black and red contours) allows identification of the PDZ residues involved in interactions with Kir2.1. The resonance position of the fully complexed PDZ (blue) is obtained from the spectrum in the presence of excess peptide fragment ^{418}EPRPLRRESEI^{428} from the C-terminus of Kir2.1. Note that the shift changes caused by Kir2.1 NC protein and peptide are collinear. (C) Comparison of the fraction of NMR resonances observed for PDZ1 and PDZ2 upon addition of increasing concentrations of KirNC. At each concentration of KirNC, the resonance intensities are normalised to the most intense and unaffected resonance from the individual C-terminus residue of the PDZ domain. (D) Comparison of the fraction of resonances observed in a sample containing a 4-fold excess (monomer concentrations) of PDZ1–3 to Kir2.1. The resonances from PDZ1, PDZ2, U3, and PDZ3 are all affected but to different extents, with PDZ2 the most and U3 the least affected, implying that PDZ2 and PDZ3, respectively, binds most strongly and weakly; K_D measurements using the isolated PDZ domains confirm these relative affinities. This experiment shows that it is possible to estimate relative binding affinities from multi-domain proteins even when line-broadening is severe; (C) and (D) are reproduced with permission from Goult et al. (2007) Biochemistry 46: 14117–14128, American Chemical Society.

$K_D < 0.1$ μM since the detection of intermolecular nOes is dependent on the lifetime of the complex. There is, however, a caveat; the larger molecular mass of the complex may preclude the observation of the nOes due to rapid transverse relaxation (line-broadening), in which case deuteration is required. For weaker complexes where the free and bound forms are in intermediate exchange, severe line-broadening will hamper detection of nOes. In the case of very weak binding, the faster off-rates and fast exchange between the free and bound forms, line-broadening in not normally an issue; in this case, it is the population of the bound species that must be considered. In theory, this can be resolve by having sufficiently high concentrations of the sample in order to increase the concentration of the bound form (Eq (4)). The structure of the Nck-3 SH3 complex in complex with PINCH-1 LIM4 (K_D is 3 mM) was determined from the intermolecular nOes obtained using half-filtered NOESY experiments and solutions containing 1.5 mM SH3 and 1 mM LIM4 [38]. In the case the complex between the cytoplasmic A and B domains of the Mannitol

Transporter II of the *Escherichia Coli* phosphoryl transferase system ($K_D \sim 3.7$ mM), the same NOESY experiments were performed in a 1:1 mixture, where each protein is at 3 mM [39].

The number of nOes between two proteins in a protein–protein complex is dependent on the binding affinity and can also be used as the first indication of the extensiveness of the binding interface. For example, in the Nck-2 SH3-3/PINCH-1 LIM4 complex with K_D 3 mM, the number of intermolecular NOE is about 31 [38]; in comparison, for the more tightly bound LynSH2-Tip complex where the K_D is 0.8 μM, over 124 intermolecular nOes were detected and used for subsequent structure calculations of the complex [40].

4.2. Cross-saturation

This dipolar cross-relaxation method identifies the protein–protein binding interface and the basis of this method is described in Fig. 4. The irradiation of protons in proton-rich protein results in proton-proton magnetisation transfer to the second, deuterated protein (and hence low-density proton) in the complex. This magnetisation transfer is measured by a change in intensity in signals in the ^{15}N–^{1}H HSQC spectrum of the second protein which is complexed to the first. Similar to nOes, this method can be used either as a direct cross-saturation or a transferred cross-saturation method dependent on the binding constant between the two proteins; a very comprehensive review of the principles and application of both approaches has been given by the originators of this technique [41].

The method requires two protein, one which is unlabelled and the other which is >99% deuterated and ^{15}N-labelled. By varying the% of D_2O in the buffer it is possible to manipulate the level of magnetisation transfer through water and reduce the overall population of the amide protons; however, the compromise is a significant decrease in sensitivity. The cross-saturation method has also been successfully applied to protein–peptide interactions [42].

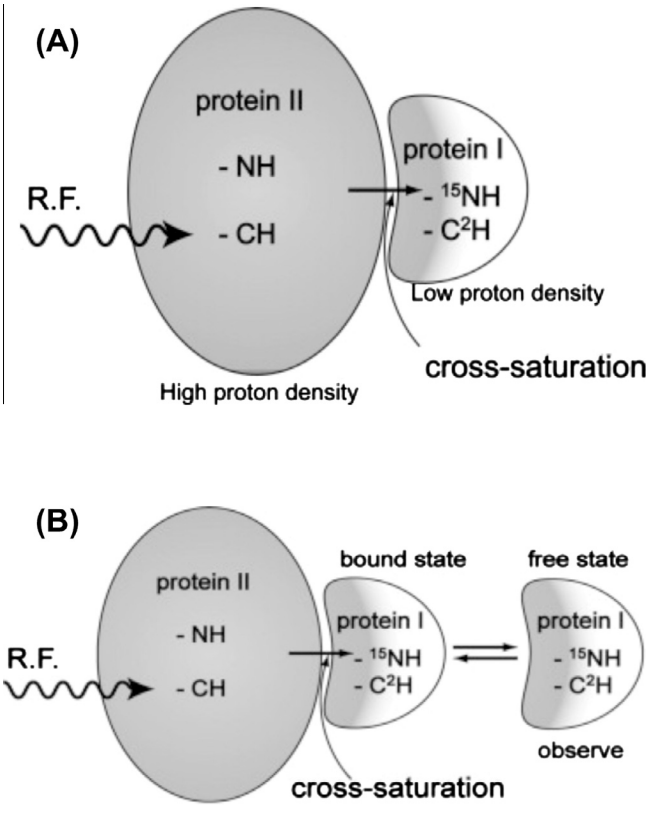

Fig. 4. In cross-saturation experiments (top), an unlabelled protein II is irradiated and the magnetisation is transferred to the bound, ^{15}N, ^{2}H labelled protein (I); residues in the binding interface from protein I are identified in this experiment. In the transferred cross-saturation method (bottom), the exchange between the free and bound protein I leads to detection of signals with reduced intensities in the free form of protein I. Reproduced with permission from Shimada et al. (2009) Prog. Nucl. Magn. Reson. Spectrosc. 54: 123–140, Elsevier.

The cross-saturation method works by directly detecting resonances from the complexed ^{15}N–^{2}H labelled protein. Often this means that the complex needs to be tight and stable, with an upper size limit of the complex that can be studied. The original method is, therefore, not suitable for large or weak complexes. The transferred cross-saturation method is a modification of the original method; rather than measuring the intensities of the fully complexed protein, the transferred method measures the intensities of resonances in the free protein, which has acquired the saturation effects from its bound form through very fast chemical exchange as depicted in Fig. 4b [43]. The efficiency of the transferred cross-relaxation experiment depends on the binding constant, the molar ratios between the two interacting proteins and the molecular weights of the two components. Through simulations, Shimada and co-workers defined conditions in which the transferred cross-saturation experiments work best [44]. These include a high mole fraction of bound ^{2}H,^{15}N protein, and fast k_{off} (>0.1 s^{-1}). Table 1 summarises the systems that have been studied using the cross-saturation experiment.

The requirement for a very high level of deuteration has been one of the main limitations of this technique. Hence, the cross-saturation method should be seen as a refinement of the chemical shift perturbation approach in order to obtain a more precise definition of the binding interface. However, it must also be remembered that the absence of a significant cross-saturation effect for a particular NH crosspeak could be due to the low proton density on the interacting surface of the other protein rather this residue not being at the binding interface.

5. Relaxation dispersion experiments

Since intermolecular interactions can affect the local and large scale motions of a protein, changes in dynamic characteristics of a protein, as determined by NMR relaxation measurements, have been used to characterise protein–protein complexes [45]. One class of experiments, the relaxation dispersion experiments, are now widely used. They have enabled the characterisation of dynamics at the micro- to millisecond (μs–ms) timescales (unlike classical NMR relaxation R_1, R_2 and heteronuclear NOE which map motions in the pico- to nanoseconds timescales which are faster than the overall correlation time). Through thorough analyses of the data, it is possible to obtain details of motions in time-averaged structures and information on conformations of lowly populated or invisible states (with at least 0.5% populations). There are many excellent reviews on the theory and applications of relaxation dispersion experiments. Palmer describes the theory of NMR characterisation of biomolecular dynamics [46]. The review by Loria et al. deals with the use of NMR relaxation dispersion measurements to characterise enzyme motions [47]. A practical overview of recent ^{15}N relaxation experiments to characterise protein dynamics is given by Ishima [48]. A more general review on the applications of relaxation dispersion experiments is given by Mittermaier and Kay [49].

Having an experiment that is capable of detecting motions in the micro- to milliseconds timescales is of significant advantage since these are timescales for catalysis, domain and loop motions, exchange between different conformations, and allosteric motions. These slow motions are also integral to the formation of protein complexes. The relaxation dispersion experiments have revealed previously inaccessible details which are relevant to enzyme

kinetics and protein function, for developing inhibitors, and defining protein folding pathways. Of most relevance to this review is the application of relaxation dispersion experiments to identify 'invisible states' [50] which are in dynamic equilibrium with more populated states during the formation of protein–protein or protein–peptide complexes.

The ability to detect 'invisible' states is of particularly relevance to titrations experiments. A majority of the NMR titrations experiments are analysed as single-step binding processes involving free and bound proteins, with no intermediate states; often this is indeed the case. However, it is possible that intermediate states are present but at very low levels or in chemical exchange with either the free or bound states and are therefore, not easily detectable. The NMR relaxation dispersion experiments allow these low-population states to be indirectly characterised through their exchange with the more highly populated forms [50,51]. Results from these analyses have revealed additional folding or interaction pathways to apparently simple processes.

In the simple model-free analyses of classical transverse relaxation times R_2, the R_{ex} term is included to account for slow chemical exchange when they are present. Hence,

$$R_2^{\text{eff}} = R_2^0 + R_{\text{ex}} \tag{7}$$

where R_2^{eff} is the measured value and is the sum of R_2^0, the intrinsic transverse relaxation rate in the absence of exchange, and R_{ex} the exchange contribution. However, the R_{ex} term does not contain details that can be used other than to indicate that there is slow exchange. The relaxation dispersion methods, on the other hand, enable more detailed characterisation of these slow exchange dynamics. The method is based on the fact that chemical exchange in the millisecond timescale being larger than the intrinsic relaxation R_2. The basic idea of relaxation dispersion experiments is to measure the variation of R_2 as a function of the effective field strength, ω_e. The applied effective field interferes with the spin dephasing due to the conformational exchange processes causing R_2 value to vary. As the larger ω_e values are more effective at suppressing the effects of conformational exchange the measured R_2 decreases with increasing ω_e [47]. Two related methods have been used to create the effective field for the T_2 measurement – Carl–Purcell–Meiboom–Gill (CPMG) and off-resonance rotating frame ($R_{1\rho}$). In the constant-time CPMG relaxation dispersion experiment, $R_{2,\text{CPMG}}$ is measured using a train of spin echo pulses and at fixed CPMG period as a function of effective field strength ω_e rad s^{-1} (or υ_{CPMG} Hz) which is related to τ_{cp}, the half-duration of CPMG interpulse delay, with $\omega_e = \pi/2\tau_{cp}$ rad s^{-1} (or $\upsilon_{\text{CPMG}} = 1/4\tau_{cp}$ Hz) [52,48]. In the off-resonance experiment, $R_{1\rho}$ is determined as a function of effective field strength ω_e by off-resonance spin-lock. Where there is no chemical exchange R_2 values will be independent of υ_{CPMG} or ω_e; when exchange is present, R_2 decreases as υ_{CPMG} or ω_e increases.

The $R_{2,\text{CPMG}}$ and $R_{1\rho}$ report on different k_{ex} values. With the CPMG experiment where the pulse repetition rate is 10^2–10^4 s^{-1}, slower timescales motions between ~50 and ~3000 events per second are measured. The $R_{1\rho}$ experiment, however, is suited for faster motions at ~1000 to ~50,000 events per second, as found in rapidly exchanging systems. To obtained reliable quantification of the chemical exchange process, it is best to match the expected timescale of the process to the particular approach. It is also desirable to have significant dispersion amplitudes. Of the two methods, the CPMG experiment is more often used. Fig. 5 summarises the chemical exchange timescales, the expected characteristics and the appropriate experiment [53]. A flat dispersion profile (where there is no variation of R_2 with υ_{CPMG} or ω_e) means that the ^{15}N chemical shifts do not experience significant fluctuations on the millisecond timescale, hence, indicating either an extremely low-level or absence of multiple conformations, an extremely rapid exchange between states (>10^4 s^{-1}), or that all the conformations share the same ^{15}N chemical shifts.

The relaxation-compensated CPMG ^{15}N relaxation dispersion data is often collected using either as an HSQC or TROSY spectrum. In the case of a two-site, fast exchange in which a single population-averaged resonance is observed, the relaxation rate constant is given by:

$$R_2^{\text{eff}}\left(\frac{1}{\tau_{cp}}\right) = R_2^0 + R_{ex}[1 - (2\tanh((k_{ex}\tau_{cp})/2))/(k_{ex}\tau_{cp})] \tag{8}$$

where $R_{ex} = p_A p_B \Delta\omega^2/k_{ex}$, p_A and p_B are equilibrium populations, k_{ex} is the sum of the forward and reverse rate constants ($k_{ex} = k_1 + k_{-1}$), τ_{cp} is the interpulse delay in the CPMG sequence, and $\Delta\omega$ is the ^{15}N chemical shift difference between the two conformations, *A* and *B*. k_{ex}, p_A and p_B, and $\Delta\omega$ between states *A* and *B* can be extracted by a fit of R_2^{eff} as a function of τ_{cp}^{-1}. Fitting is often performed using programmes such as CPMGFit [54] and NESSY [55].

For weak protein–protein interactions, relaxation dispersion approaches have been used to understand in greater detail the mechanism(s) of interactions and the determination of the structures of intermediates in interaction pathways which are often in low population and are hence 'invisible'. A good example of a weak protein–protein interaction is the binding between CIN85 SH3 and ubiquitin. While NMR chemical shift titration of alternately ^{15}N-labelled ubiquitin and ^{15}N-labelled CIN85 SH3 with the unlabelled partner yielded K_D values of 167 and 215 μM respectively, relaxation dispersion measurements and global curve fit gave K_D values 2.9 mM and 3.7 mM, for, respectively, ^{15}N ubiquitin and ^{15}N SH3 domain [56]. This discrepancy was reconciled by using a three-state rather than a simple two-state binding model. This example highlights how apparently simple interactions between two entities can in fact involve a complex interplay between entropy and enthalpy, obtained through a careful analysis of relaxation dispersion data supplemented by results from isothermal titration calorimetry ITC experiments.

The strength of the relaxation dispersion method is that, in principle, it is possible to obtain the chemical positions of species which cannot be observed either because of extreme line-broadening effects or low population. Hansen et al. [51,57,58] demonstrates this using the SH3-peptide complex (K_D of 0.55 μM). They validated the reliability of relaxation dispersion to provide chemical shift information by showing that the chemical shifts extracted

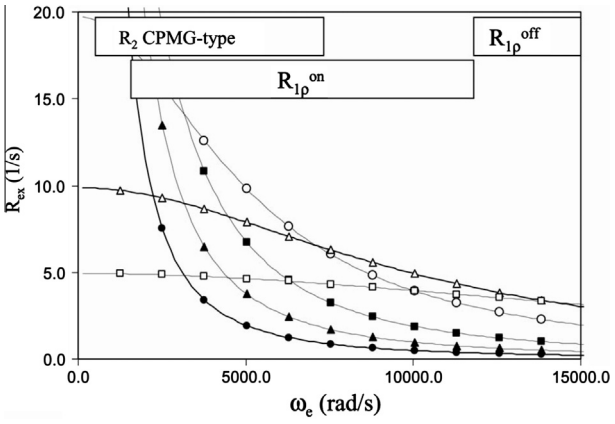

Fig. 5. Theoretical representation of the chemical exchange contribution as a function of effective field strengths ω_e rad s^{-1} for a two-site conformational exchange at different exchange timescales. Shown in the figure is the range of effective field strengths over which the different relaxation experiments are suitable. Reproduced with permission from Kim and Baum (2004) J. Biom. NMR. 30: 195–204, Springer.

from the relaxation dispersion experiments are almost entirely consistent those directly measured. This opens up the possibility that structures of lowly-populated states will in future be forthcoming.

6. Paramagnetic effects

Unpaired electrons have strong magnetic moments and can dramatically affect nearby nuclei because of the dipolar interaction between the electron and nucleus. A nuclear resonance can be broadened (relaxation effects) or shifted and these paramagnetic effects are dependent on distance and orientation. Examples of NMR parameters induced by paramagnetism include paramagnetic relaxation enhancement (PRE), pseudocontact shifts (PCS), paramagnetically-induced residual dipolar couplings (RDCs) and Curie-dipolar cross-correlated relaxation. PREs can be detected in any paramagnetic system; PCSs and RDCs, on the other hand, can only be observed with an anisotropic electron g-factor [22]. Paramagnetic effects are experienced over a long-range of approximately 60 Å and are, hence, particularly suitable for studying non-covalent complexes.

Encounter complexes, including the electron transfer systems, are prime examples of transient complexes and the paramagnets, found naturally or introduced into these proteins, have been used in NMR to provide invaluable structural information. Paramagnetic effects, their theory, practice and applications have been comprehensively reviewed [22,59,60]. Ubbink gives a good overview of how paramagnetic effects have been applied to the redox complexes [61] and highlights that some complexes exist as non-specific, dynamic conformational ensembles while others are more stable and assume single orientations [62]. The review by Bertini et al. provides another perspective of paramagnetic NMR of metalloproteins by focusing on ^{13}C direct detection NMR [63].

NMR paramagnetic effects are well known since the discovery of NMR. It is the focused study of a few systems, such as the protein–protein electron transfer encounter complexes [64] and the resultant development of the theoretical and computational framework for the quantitative analysis of paramagnetic relaxation rates that have led to the recent exploitation of the NMR paramagnetic effects in more sophisticated ways [22]. The applications that have arisen from these theoretical developments have enabled paramagnetic relaxation rates to be used more reliably for structure determination and also for detailed analysis of low population states that are in fast exchange with major species, such as in encounter complexes [65,66].

The presence of a paramagnet will increase the *longitudinal* and *transverse* relaxation rates. The difference in relaxation rates in the presence and absence of the paramagnet is referred to as the paramagnetic relaxation enhancement (PRE). In paramagnetic systems, the correlation time, τ_c, is defined as $(\tau_r^{-1} + \tau_s^{-1})$, where τ_r^{-1} is the correlation time of the macromolecule and τ_s^{-1} is the effective electronic correlation time. For most proteins, τ_r^{-1} is >5 ns, and τ_s^{-1} dominates and the *longitudinal* relaxation rate enhancement is related to the distance between the nucleus and a paramagnet as given by the simplified equation:

$$R_1^{\text{para}} = \frac{2}{15}\left(\frac{\mu_0}{4\pi}\right)^2 \frac{\gamma_I^2 g_e^2 \mu_B^2 S(S+1)}{r_{IM}^6}\left(\frac{7\tau_s}{1+\omega_S^2\tau_s^2} + \frac{3\tau_S}{1+\omega_I^2\tau_s^2}\right) \quad (9)$$

More commonly used, however, is the paramagnetic *transverse* relaxation of a nucleus, which is also related to the distance between the paramagnet and nucleus and in its simplified form is given as:

$$R_2^{\text{para}} = \frac{1}{15}\left(\frac{\mu_0}{4\pi}\right)^2 \frac{\gamma_I^2 g_e^2 \mu_B^2 S(S+1)}{r_{IM}^6}\left(4\tau_C + \frac{3\tau_S}{1+\omega_I^2\tau_c^2}\right) \quad (10)$$

The symbols and physical constants are defined as: τ_S electron relaxation time, correlation time, μ_0 permeability of vacuum, μ_B Bohr constant, γ_I gyromagnetic ratio of nuclei I, g_e electronic g-factor, S spin quantum number, r_{IM}, nucleus metal distance, ω_I, ω_S the Larmor frequencies of, respectively, nucleus I and S. As can be seen from the equations, the PRE is a highly sensitive effect which decreases as the sixth power of the electron-nucleus distance. PREs are particularly suited for detecting (and characterising) the low population states and have been successfully exploited to study weak and transient associations between macromolecules where there is rapid exchange between the nuclei and paramagnetic centres (>1000 s per second). In the fast exchange regime, the observed experimental PREs are population-weighted averages of the PREs over the various conformational states. Hence, even if the paramagnetic label is in close proximity for only a very small fraction of the time, the PREs for this state makes a measurable contribution to the experimental relaxation rates. Therefore, the PRE observed is related to the distance from the unpaired electron as well as the relative populations (relaxation enhanced vs. non-enhanced) of the different states.

Stable unpaired electrons are found in metals and radicals. Two general classes of paramagnetic probes are commonly used in NMR: paramagnetic metals and chemical probes, the latter broadly divided into (i) nitroxide stable radicals, (ii) synthetic metal chelators (such as ethylenediaminetetraacetic acid (EDTA), diethylene triamine pentaacetic acid (DTPA) and metal binding peptides), and (iii) metal-binding peptides [22]. Paramagnetic metals are present in proteins, either naturally as cofactors Fe^{3+}, Cu^{2+}, or as substitutes (Mn^{2+}, Co^{2+}, caged lanthanides). Examples of metal proteins for which NMR has been extensively used include the copper proteins plastocyanin [67] and azurin [68]. Lanthanides do not exist naturally in proteins but can be readily exchanged for Ca^{2+} and Mg^{2+}.

The paramagnetic chemical probes can be covalently attached to proteins and used for the observation of intramolecular and intermolecular PREs. The probes are most often covalently attached to the protein termini or to solvent exposed cysteine residues which are present naturally or can be readily introduced by site-directed mutagenesis. In addition, free probes, such as small compounds containing paramagnetic centres, can be added to a protein solution as co-solutes and these are useful for identifying solvent accessible regions [69]. Table 1 summarises the major systems for which paramagnetic tools have been used.

The structural characterisation of low population species formed during the early stages of protein–protein interactions was described for the bacterial phosphotransferase system using detailed analyses of the paramagnetic relaxation effects, which included a comparison between experimentally-derived and back-calculated paramagnetic T_2 values from known structures [70]. More recently, a titration experiment [66] was used to obtain very detailed information on this complex. In this experiment the ^{15}N-labelled N-terminal domain of Enzyme I (EIN) was titrated with the EDTA-Mn^{2+} conjugated to HPr via three cysteine sites; the complex has a $K_D \sim 5$ μM. The exchange between the specific complex, non-specific encounter complex species and the free, dissociated proteins was fast on the chemical shift and PRE relaxation timescales. allowing the intermolecular PRE to report on the transient species. By analysing the concentration-dependence of PRE effects of individual amino acids on EIN, it was possible to reveal the presence of specific and non-specific encounter complexes. Within the latter group, a further classification into several different, coexisting, configurations was achieved (Fig. 6).The results obtained provided a detailed description of the species that could exist along the EIN-HPR association pathway.

The yeast cytochrome c and yeast cytochrome c peroxidise complex binds with a $K_D \sim 5$ μM [71] and has been a paradigm

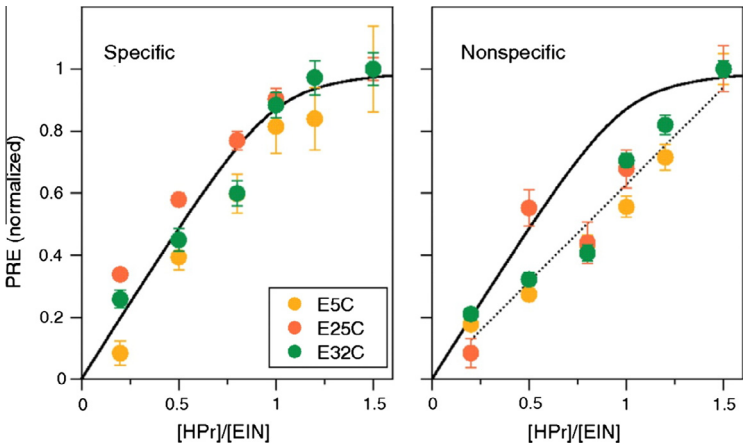

Fig. 6. Intermolecular paramagnetic relaxation enhancements (PRE) on $^{15}N/^{2}H$-labelled N-terminal domain of Enzyme Complex I (EIN) performed at different concentrations of paramagnetically labelled (EDTA-Mn^{2+}-tagged) histidine-containing phosphocarrier protein (HPr) at molar ratios 0.2–1.5. HPr is separately tagged in three different sites (E5C, E25C and E32C) to provide probes that will detect specific complexes and non-specific encounter complexes. The left-hand panel shows specific PREs where there is saturation as the HPr concentration exceeds the EIN concentration and the normalised PREs fit to a simple two-site binding with $K_D \sim 7$ μM. The right hand panel shows nonspecific intermolecular PREs since the titration curves deviate significantly from a simple two-site binding model. The black line in both panels show the curve fit. The data shows the presence of at least two populations whose PRE titration behaviours are distinct from each other. Reproduced with permission from Fawzi et al. (2010) Proc. Natl. Acad. Sci. U.S.A. 107: 1379–1384.

for intermolecular electron transfer (ET) [72] with both the crystal [73] and NMR [65] structures being available. This transient, electron transfer complex is dynamic. The NMR studies showed that the dominant, ET-active protein–protein orientation, as determined by NMR and X-ray crystallography, was occupied >70% of the lifetime of the complex, with the rest of the time being spent as an ensemble of structures, representing the encounter complexes. The structure of the complex was calculated using protein docking and energy minimisation, incorporating the intermolecular distance restraints afforded by the PRE effects on cytochrome c caused by the paramagnetic nitroxide spin label, (1-oxyl-2,2,5,5-tetramethyl-3-pyrroline-3-methyl)-methanethiosulfonate (MTSL) which was covalently attached to the partner protein, cytochrome c peroxidise [65]. While most of the PRE-derived restraints were satisfied in the resulting model, there were some that were violated although these were not randomly distributed. The concentration independent characteristics of these additional PREs and its localised nature suggested that multiple-protein–protein orientations existed. More detailed analysis of these paramagnetic effects, combined with information from other studies, led to the conclusion that the forward and backward electron transfer rates were differentially modulated, with the forward electron transfer rates being conformationally gated. Other protein heterotypic complexes for which NMR paramagnetic effects having been used are summarised in Table 1.

7. Residual dipolar coupling

The dipolar interaction (coupling) between two nuclei gives rise to a splitting of the NMR resonance which is dependent of the distance between the two nuclei and the orientation of their inter-nuclear vector relative to the applied magnetic field. Dipolar couplings average to zero when the protein tumbles isotropically in solution. Residual dipolar couplings (RDCs) can be reintroduced by the partial alignment of the macromolecule in an anisotropic manner. This is normally done by the addition of anisotropic media such as liquid crystals, filamentous phage, bicelles or by polyacrylamide gels. The $^{15}N–^{1}H$ residual dipolar coupling is most commonly measured using the $^{15}N–^{1}H$ HSQC spectrum. The small dipolar splitting (tens of Hertz) that can be measured provides information of how the bond vector between the observed nuclei are aligned to the external magnetic field. Effectively, this gives information as to how the bond vectors are orientated relative to each other and enables the molecular alignment tensor of the molecule to be determined. After NOE, restraints derived from residual dipolar couplings are the most common NMR restraints for NMR structure calculations. The review by Jensen et al. focuses on the use of residual dipolar for the characterisation of weak protein–protein complexes [74].

Due to the inherent insensitivity of the NOE experiments in weakly-binding complexes, RDC used as restraints for determining the structures of these complexes are becoming increasingly important. By measuring the RDC for each component in a protein–protein complex, it is possible, in principle, to calculate the orientations of the two proteins relative to each other. However, in cases of weak binding and fast exchange between the free and bound forms, it is necessary to bear in mind that the measured RDC, like measured average chemical shifts, is the population-weighted average of the RDCs in the free and fully-bound form. It is, hence, important that the alignment characteristics of the free and bound forms of both partners in the complex be determined and alignment levels properly and accurately calibrated. A similar analysis as used for the chemical shift perturbation needs to be undertaken, with RDC of the bound form obtained indirectly by extrapolation of the RDCs at different points in a titration. If the molar ratio of the bound and free forms of a protein (from the K_D values and molar concentrations of the free and complexed form) and the RDCs for the free form are known, it is possible to calculate the RDC for the bound form:

$$D_{ij}^{\text{bound}} = \left(D_{ij}^{\text{measured}} - X^{\text{free}} D_{ij}^{\text{free}}\right) \Big/ X^{\text{bound}} \tag{11}$$

where D_{ij} is the RDC value between nuclei i and j, X^{free}, X^{bound} are, respectively, the molar ratio of the free and bound forms of the protein [74]. This indirect method of obtaining the RDC of the bound form avoids the need to use very high concentrations of the partner protein in order to achieve saturation of the observed, labelled protein.

Ortega-Roldan et al. [24] showed, using the CD2AP SH3-C:ubiquitin complex system, an RDC titration approach which gives good, robust estimations of the RDC values of the bound forms in weak complexes. The approach described works provided both proteins

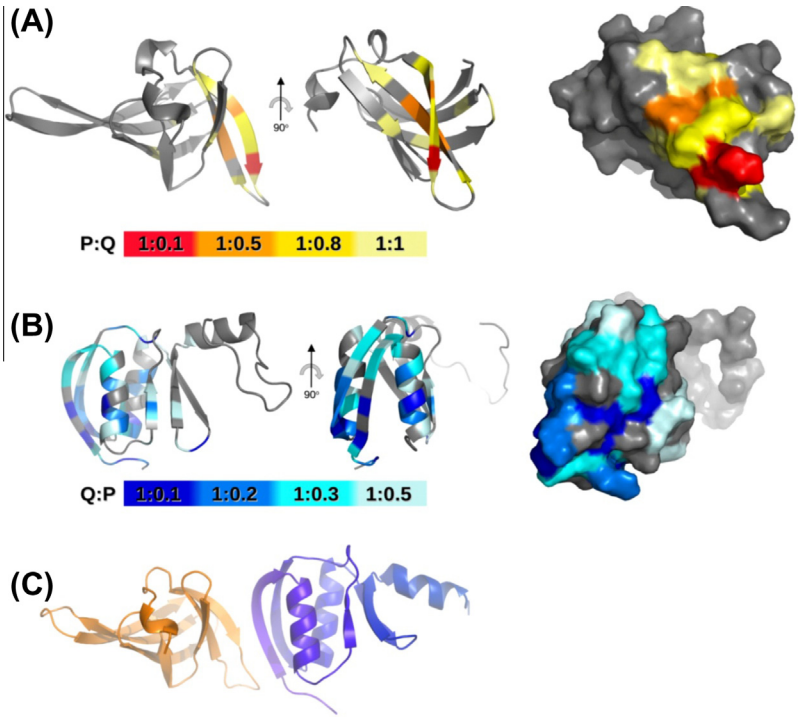

Fig. 7. Structural model for the PilP C-domain bound to the PilQ N0 domain. (A) Decrease is peak intensities mapped onto the PilP C-domain (PDB accession 2IVW) following titration with N0N1PilQ$^{343-545}$. Ratios of PilP:PilQ were coloured as follows: 1:0.1, red; 1:0.5, orange; 1:0.8, yellow; 1:1, pale-yellow. Left, ribbon plot with β1 stand marked; right, surface plot. (B) Decrease in peak intensities mapped onto NmPilQ$^{343-442}$. Ratios of PilQ:PilP were coloured as follows: 1:0.1, dark-blue; 1:0.2, blue; 1:0.3, cyan; 1:0.5, pale-blue. (C) Model of the PilP$^{77-164}$: N0PilQ$^{343-442}$ complex generated from the chemical shift perturbations shown in (A) and (B) using HADDOCK [20] followed by CNS1.2 [77] with PilP$^{77-164}$ in gold and N0PilQ$^{343-442}$ in blue [100].

and the complex can be successfully aligned in the same medium. The use of RDCs in weak protein–protein complexes can be problematic even when alignment media are found because of the differential interaction of one partner with the alignment medium. Similarly, the high concentrations needed to increase the population of the complexed form can cause molecular crowding, giving rise to differential perturbation of the alignment tensor by the unlabelled protein [39].

8. Modelling of weak protein–protein complexes

High-resolution structures of weak heterotypic protein–protein complexes are difficult to determine because there are often insufficient structural restraints for a full structure determination. Hence, at best, a structural model which appropriately describes the most populated complex, and which satisfies an array of intermolecular restraints, can be obtained. These models are obtained by incorporating the experimental restraints into structure calculations programmes such as HADDOCK which was developed by Bonvin and his colleagues [20,75]. HADDOCK works on the basis that it uses ambiguous interaction restraints (AIRs) between amino acid residues which are defined as forming the interaction interface for the structure calculations. Chemical shift perturbations (and mutagenesis based on CSP), relaxation data paramagnetic relaxation enhancements, deuterium exchange, residual dipolar couplings and mutagenesis are some of the NMR experiments used to obtain the AIRs [19,76]. Apart from its flexibility in being able to use restraints from different sources and experiments, the strength of the HADDOCK method is that it allows increasing levels of flexibility through the docking procedure; a good account of HADDOCK and other protein docking methods is given in Ref. [18]. Over 92 HADDOCK models of protein complexes have been deposited in the Protein Data Bank, demonstrating the power of this approach.

Often, chemical shift perturbations are the only restraints available to model the protein–protein complex using HADDOCK. To get a more reliable complex structure, it may be necessary to adopt a 2-stage approach where the HADDOCK method is used in combination with other programmes. An example of this is the determination of the structure of the weak complex between PilP$^{77-164}$ and the N0N1 domains of PilQ which is a component of the trans-periplasmic channel assembly of the Type IV Pili in *Neisseria meningitides* (K_D in the high micormolar range) [100]. The structure of the complex was initially modelled using HADDOCK. Comparison of this model with a related complex whose crystal is known revealed that one side-chain in the PilP$^{77-164}$-N0N1 HADDOCK structure was artificially fixed in position by the rigid body docking procedure, leading to differences between the structure of PilP$^{77-164}$-N0N1 complex and the crystal structure. Using the hydrogen bond interactions identified from the initial HADDOCK structures, together with the chemical shift perturbation restraints, a further structure refinement using Crystallography and NMR System (CNS) version 1.2 [77] was performed to generate the final model which is a better match to the determined crystal structure (Fig. 7). Also shown in the figure are the chemical shift perturbations upon titration of one protein into the other (add reference).

9. Conclusion and perspective

Weak protein–protein complexes constitute a significant proportion of biological interactions, being essential for mediating and regulating many processes and pathways. These interactions may either form the initial part of a stable, strong interaction or are transient interactions such as those found in electron transfer systems. Detecting, quantifying and characterising these weak interactions is challenging because of partly the dynamic nature, and the low population levels, of the complexes. NMR is proving to be a very successful method in not only detecting the presence

of low populations of the complex, but also in quantifying the dynamic motions, determining affinity constants and in producing structures of protein–protein complexes. The success of many of the techniques currently being used for the characterisation of these weak complexes is predominantly due to the significant efforts undertaken to exploit the various NMR experiments that were originally designed for other purposes, in particular for high-resolution structure determination. These developments have led to some very elegant elucidation of interaction pathways and mechanisms not previously revealed by other methods and to the characterisation of low population species. NMR, as a tool for the identification of interaction interface in weak complexes, has been extremely successful and the results of these experiments have opened up new avenues of research. The corollary is that a failure by NMR to detect interactions which had been previously been observed or deduced from other experiments has led to more confirmatory work being performed and sometimes a revision of hypotheses. The characteristics of weak interactions – low affinities, fast k_{off}, slow dynamics, low populations – are all amenable for detailed studies by NMR. Finally, the detailed characterisation of some of the weak interactions, in conjunction with other biological studies, has and can lead to the identification of potential therapeutic targets for many disease states Therefore, NMR will remain one of the major techniques for the detailed studies of weak protein–protein complexes.

References

[1] I.M.A. Nooren, J.M. Thornton, Diversity of protein-protein interactions, EMBO J. 22 (2003) 3486–3492.
[2] I.M.A. Nooren, J.M. Thornton, Structural characterisation and functional significance of transient protein-protein interactions, J. Mol. Biol. 325 (2003) 991–1018.
[3] M. Schlosshauer, D. Baker, Realistic protein-protein association rates from a simple diffusional model neglecting long-range interactions, free energy barriers, and landscape ruggedness, Protein Sci. 13 (2004) 1660–1669.
[4] A.J. Rowe, Ultra-weak reversible protein-protein interactions, Methods 54 (2011) 157–166.
[5] K. Henzler-Wildman, D. Kern, Dynamic personalities of proteins, Nature 450 (2007) 964–972.
[6] J.E. Ladbury, M.A. Williams, The extended interface. measuring non-local effects in biomolecular interactions, Curr. Opin. Struc. Biol. 14 (2004) 562–569.
[7] A. Bonvin, R. Boelens, R. Kaptein, NMR analysis of protein interactions, Curr. Opin. Chem. Biol. 9 (2005) 501–508.
[8] P. Foster, A. McElroy, C.D. Amero, Solution NMR of large molecules and assemblies, Biochemistry 46 (2007) 331–340.
[9] C.J. Markin, X.A. Wei, L. Spyracopoulos, Mechanism for recognition of polyubiquitin chains: balancing affinity through interplay between multivalent binding and dynamics, J. Am. Chem. Soc. 132 (2010) 11247–11258.
[10] M.R. O'Connell, R. Gamsjaeger, J.P. Mackay, The structural analysis of protein-protein interactions by NMR spectroscopy, Proteomics 9 (2009) 5224–5232.
[11] T. Stangler, R. Hartmann, D. Willbold, B.W. Koenig, Modern high resolution NMR for the study of structure, dynamics and interactions of biological macromolecules, Zeitschrift Fur Physikalische Chemie – Int. J. Res. Phys. Chem. Chem. Phys. 220 (2006) 567–613.
[12] J. Vaynberg, J. Qin, Weak protein-protein interactions as probed by NMR spectroscopy, Trends Biotechnol. 24 (2006) 22–27.
[13] O. Vinogradova, J. Qin, NMR as a unique tool in assessment and complex determination of weak protein-protein interactions, Top. Curr. Chem. 326 (2012) 35–45.
[14] E.R.P. Zuiderweg, Mapping protein-protein interactions in solution by NMR Spectroscopy, Biochemistry 41 (2002) 1–7.
[15] L. Fielding, NMR methods for the determination of protein-ligand dissociation constants, Prog. Nucl. Magn. Reson. Spectrosc. 51 (2007) 219–242.
[16] J.P. Demers, A. Mittermaier, Binding Mechanism of an SH3 Domain Studied by NMR and ITC, J. Am. Chem. Soc. 131 (2009) 4355–4367.
[17] G.M. Clore, Accurate and rapid docking of protein-protein complexes on the basis of intermolecular nuclear Overhauser enhancement data and dipolar couplings by rigid body minimization, Proc. Natl. Acad. Sci. USA 97 (2000) 9021–9025.
[18] A.D.J. van Dijk, R. Boelens, A. Bonvin, Data-driven docking for the study of biomolecular complexes, FEBS J. 272 (2005) 293–312.
[19] A.D.J. van Dijk, R. Kaptein, R. Boelens, A. Bonvin, Combining NMR relaxation with chemical shift perturbation data to drive protein-protein docking, J. Biomol. NMR 34 (2006) 237–244.
[20] S.J. De Vries, M. van Dijk, A. Bonvin, The HADDOCK web server for data-driven biomolecular docking, Nat. Protoc. 5 (2010) 883–897.
[21] J. Iwahara, G.M. Clore, Detecting transient intermediates in macromolecular binding by paramagnetic NMR, Nature 440 (2006) 1227–1230.
[22] G.M. Clore, J. Iwahara, Theory, practice, and applications of paramagnetic relaxation enhancement for the characterization of transient low-population states of biological macromolecules and their complexes, Chem. Rev. 109 (2009) 4108–4139.
[23] G.M. Clore, Exploring sparsely populated states of macromolecules by diamagnetic and paramagnetic NMR relaxation, Protein Sci. 20 (2011) 229–246.
[24] J.L. Ortega-Roldan, M.R. Jensen, B. Brutscher, A.I. Azuaga, M. Blackledge, N.A.J. van Nuland, Accurate characterization of weak macromolecular interactions by titration of NMR residual dipolar couplings: application to the CD2AP SH3-C:ubiquitin complex, Nucleic Acids Res. 37 (2009).
[25] L. Salmon, J.L.O. Roldan, E. Lescop, A. Licinio, N. van Nuland, M.R. Jensen, M. Blackledge, Structure, dynamics, and kinetics of weak protein-protein complexes from NMR spin relaxation measurements of titrated solutions, Angew. Chem. Int. Ed. 50 (2011) 3755–3759.
[26] L.Y. Lian, G.C.K. Roberts, Protein NMR Spectroscopy: Principal Techniques and Applications, Wiley, 2010.
[27] L.Y. Lian, D.A. Middleton, Labelling approaches for protein structural studies by solution-state and solid-state NMR, Prog. Nucl. Magn. Reson. Spectrosc. 39 (2001) 171–190.
[28] M. Tonelli, L.R. Masterson, G. Cornilescu, J.L. Markley, G. Veglia, One-sample approach to determine the relative orientations of proteins in ternary and binary complexes from residual dipolar coupling measurements, J. Am. Chem. Soc. 131 (2009) 14138–14139.
[29] A.P. Golovanov, R.T. Blankley, J.M. Avis, W. Bermel, Isotopically discriminated NMR spectroscopy: a tool for investigating complex protein interactions in vitro, J. Am. Chem. Soc. 129 (2007) 6528–6535.
[30] W. Bermel, E.N. Tkach, A.G. Sobol, A.P. Golovanov, Simultaneous measurement of residual dipolar couplings for proteins in complex using the isotopically discriminated NMR approach, J. Am. Chem. Soc. 131 (2009) 8564–8570.
[31] B.T. Goult, J.D. Rapley, C. Dart, A. Kitmitto, J.G. Grossmann, M.L. Leyland, L.-Y. Lian, Small-angle X-ray scattering and NMR studies of the conformation of the PDZ region of SAP97 and its interactions with Kir2.1, Biochemistry 46 (2007) 14117–14128.
[32] C. de Chiara, R.P. Menon, A. Pastore, Structural bases for recognition of Anp32/LANP proteins, FEBS J. 275 (2008) 2548–2560.
[33] I. Bezsonova, M.C. Bruce, S. Wiesner, H. Lin, D. Rotin, J.D. Forman-Kay, Interactions between the three CIN85SH3 domains and ubiquitin: Implications for CIN85 ubiquitination, Biochemistry 47 (2008) 8937–8949.
[34] C. Ma, W. Li, Y.B. Xu, J. Rizo, Munc13 mediates the transition from the closed syntaxin-Munc18 complex to the SNARE complex, Nat. Struct. Mol. Biol. 18 (2011) 542–549.
[35] S. Pegan, J. Tan, A. Huang, P.A. Slesinger, R. Riek, S. Choe, NMR studies of interactions between C-terminal tail of Kir2.1 channel and PDZ1,2 domains of PSD95, Biochemistry 46 (2007) 5315–5322.
[36] L.Y. Lian, I.L. Barsukov, M.J. Sutcliffe, K.H. Sze, G.C.K. Roberts, Protein ligand interactions – exchange processes and determination of ligand conformation and protein-ligand contacts, Methods Enzymol. 239 (1994) 657–700.
[37] K.J. Walters, H. Matsuo, G. Wagner, A simple method to distinguish intermonomer nuclear overhauser effects in homodimeric proteins with C-2 symmetry, J. Am. Chem. Soc. 119 (1997) 5958–5959.
[38] J. Vaynberg, T. Fukuda, K. Chen, O. Vinogradova, A. Velyvis, Y.Z. Tu, L. Ng, C.Y. Wu, J. Qin, Structure of an ultraweak protein-protein complex and its crucial role in regulation of cell morphology and motility, Mol. Cell 17 (2005) 513–523.
[39] J.Y. Suh, M.L. Cai, D.C. Williams, G.M. Clore, Solution structure of a post-transition state analog of the phosphotransfer reaction between the A and B cytoplasmic domains of the mannitol transporter IIMannitol of the *Escherichia coli* phosphotransferase system, J. Biol. Chem. 281 (2006) 8939–8949.
[40] F. Bauer, K. Schweimer, H. Meiselbach, S. Hoffmann, P. Rosch, H. Sticht, Structural characterization of Lyn-SH3 domain in complex with a herpesviral protein reveals an extended recognition motif that enhances binding affinity, Protein Sci. 14 (2005) 2487–2498.
[41] I. Shimada, T. Ueda, M. Matsumoto, M. Sakakura, M. Osawa, K. Takeuchi, N. Nishida, H. Takahashi, Cross-saturation and transferred cross-saturation experiments, Prog. Nucl. Magn. Reson. Spectrosc. 54 (2009) 123–140.
[42] J. Morrison, J.C. Yang, M. Stewart, D. Neuhaus, Solution NMR study of the interaction between NTF2 and nucleoporin FxFG repeats, J. Mol. Biol. 333 (2003) 587–603.
[43] T. Nakanishi, M. Miyazawa, M. Sakakura, H. Terasawa, H. Takahashi, I. Shimada, Determination of the interface of a large protein complex by transferred cross-saturation measurements, J. Mol. Biol. 318 (2002) 245–249.
[44] M. Matsumoto, T. Ueda, I. Shimada, Theoretical analyses of the transferred cross-saturation method, J. Magn. Reson. 205 (2010) 114–124.
[45] R.A. Atkinson, B. Kieffer, The role of protein motions in molecular recognition: insights from heteronuclear NMR relaxation measurements, Prog. Nucl. Magn. Reson. Spectrosc. 44 (2004) 141–187.
[46] A.G. Palmer, NMR characterization of the dynamics of biomacromolecules, Chem. Rev. 104 (2004) 3623–3640.
[47] J.P. Loria, R.B. Berlow, E.D. Watt, Characterization of enzyme motions by solution NMR relaxation dispersion, Acc. Chem. Res. 41 (2008) 214–221.

[48] R. Ishima, Recent developments in (15)N NMR relaxation studies that probe protein backbone dynamics, Top. Curr. Chem. 326 (2012) 99–122.
[49] A.K. Mittermaier, L.E. Kay, Observing biological dynamics at atomic resolution using NMR, Trends Biochem. Sci. 34 (2009) 601–611.
[50] D.M. Korzhnev, X. Salvatella, M. Vendruscolo, A.A. Di Nardo, A.R. Davidson, C.M. Dobson, L.E. Kay, Low-populated folding intermediates of Fyn SH3 characterized by relaxation dispersion NMR, Nature 430 (2004) 586–590.
[51] D.F. Hansen, P. Vallurupalli, L.E. Kay, Using relaxation dispersion NMR spectroscopy to determine structures of excited, invisible protein states, J. Biomol. NMR 41 (2008) 113–120.
[52] R. Ishima, D.A. Torchia, Estimating the time scale of chemical exchange of proteins from measurements of transverse relaxation rates in solution, J. Biomol. NMR 14 (1999) 369–372.
[53] S. Kim, J. Baum, An on/off resonance rotating frame relaxation experiment to monitor millisecond to microsecond timescale dynamics, J. Biomol. NMR 30 (2004) 195–204.
[54] A. Palmer III, CPMG FIT.
[55] M. Bieri, P.R. Gooley, Automated NMR relaxation dispersion data analysis using NESSY, BMC Bioinf. 12 (2011).
[56] D.M. Korzhnev, I. Bezsonova, S. Lee, T.V. Chalikian, L.E. Kay, Alternate binding modes for a ubiquitin-SH3 domain interaction studied by NMR spectroscopy, J. Mol. Biol. 386 (2009) 391–405.
[57] D.F. Hansen, P. Vallurupalli, P. Lundstrom, P. Neudecker, L.E. Kay, Probing chemical shifts of invisible states of proteins with relaxation dispersion NMR spectroscopy: how well can we do?, J Am. Chem. Soc. 130 (2008) 2667–2675.
[58] P. Vallurupalli, D.F. Hansen, L.E. Kay, Structures of invisible, excited protein states by relaxation dispersion NMR spectroscopy, Proc. Natl. Acad. Sci. USA 105 (2008) 11766–11771.
[59] G.M. Clore, C. Tang, J. Iwahara, Elucidating transient macromolecular interactions using paramagnetic relaxation enhancement, Curr. Opin. Struct. Biol. 17 (2007) 603–616.
[60] G.M. Clore, Visualizing lowly-populated regions of the free energy landscape of macromolecular complexes by paramagnetic relaxation enhancement, Mol. Biosyst. 4 (2008) 1058–1069.
[61] M. Ubbink, Complexes of photosynthetic redox proteins studied by NMR, Photosynth. Res. 81 (2004) 277–287.
[62] M. Prudencio, M. Ubbink, Transient complexes of redox proteins: structural and dynamic details from NMR studies, J. Mol. Recognit. 17 (2004) 524–539.
[63] I. Bertini, C. Luchinat, G. Parigi, R. Pierattelli, Perspectives in paramagnetic NMR of metalloproteins, Dalton Trans. (2008) 3782–3790.
[64] M. Ubbink, The courtship of proteins: Understanding the encounter complex, FEBS Lett. 583 (2009) 1060–1066.
[65] A.N. Volkov, J.A.R. Worrall, E. Holtzmann, M. Ubbink, Solution structure and dynamics of the complex between cytochrome c and cytochrome c peroxidase determined by paramagnetic NMR, Proc. Natl. Acad. Sci. USA 103 (2006) 18945–18950.
[66] N.L. Fawzi, M. Doucleff, J.Y. Suh, G.M. Clore, Mechanistic details of a protein-protein association pathway revealed by paramagnetic relaxation enhancement titration measurements, Proc. Natl. Acad. Sci. USA 107 (2010) 1379–1384.
[67] M. Ubbink, M. Ejdeback, B.G. Karlsson, D.S. Bendall, The structure of the complex of plastocyanin and cytochrome f, determined by paramagnetic NMR and restrained rigid-body molecular dynamics, Structure 6 (1998) 323–335.
[68] A. Impagliazzo, M. Ubbink, Mapping of the binding site on pseudoazurin in the transient 152 kDa complex with nitrite reductase, J. Am. Chem. Soc. 126 (2004) 5658–5659.
[69] A.P. Golovanov, T.H. Chuang, C. DerMardirossian, I. Barsukov, D. Hawkins, R. Badii, G.M. Bokoch, L.Y. Lian, G.C.K. Roberts, Structure-activity relationships in flexible protein domains: regulation of rho GTPases by RhoGDI and D4 GDI, J. Mol. Biol. 305 (2001) 121–135.
[70] C. Tang, J. Iwahara, G.M. Clore, Visualization of transient encounter complexes in protein-protein association, Nature 444 (2006) 383–386.
[71] A.N. Volkov, O. Bashir, J.A.R. Worrall, M. Ubbink, Binding hot spot in the weak protein complex of physiological redox partners yeast cytochrome c and cytochrome c peroxidase, J. Mol. Biol. 385 (2009) 1003–1013.
[72] A.N. Volkov, P. Nicholls, J.A.R. Worrall, The complex of cytochrome c and cytochrome c peroxidase: The end of the road?, Biochim Biophys. Acta Bioenerg. 1807 (2011) 1482–1503.
[73] H. Pelletier, J. Kraut, Crystal structure of a complex between electron-transfer partners, cytochrome c peroxidase and cytochrome c, Science 258 (1992) 1748–1755.
[74] M.R. Jensen, J.L. Ortega-Roldan, L. Salmon, N. van Nuland, M. Blackledge, Characterizing weak protein-protein complexes by NMR residual dipolar couplings, Eur. Biophys. J. 40 (2011) 1371–1381.
[75] C. Dominguez, R. Boelens, A. Bonvin, HADDOCK: a protein-protein docking approach based on biochemical or biophysical information, J. Am. Chem. Soc. 125 (2003) 1731–1737.
[76] A.D.J. van Dijk, S. Ciofi-Baffoni, L. Banci, I. Bertini, R. Boelens, A. Bonvin, Modeling protein-protein complexes involved in the cytochrome c oxidase copper-delivery pathway, J. Proteome Res. 6 (2007) 1530–1539.
[77] A.T. Brunger, Version 1.2 of the Crystallography and NMR system, Nat. Protoc. 2 (2007) 2728–2733.
[78] Y. He, L. Hicke, I. Radhakrishnan, Structural basis for ubiquitin recognition by SH3 domains, J. Mol. Biol. 373 (2007) 190–196.
[79] S. McKenna, J. Hu, T. Moraes, W. Xiao, M.J. Ellison, L. Spyracopoulos, Energetics and specificity of interactions within Ub center dot Uev center dot Ubc13 human ubiquitin conjugation complexes, Biochemistry 42 (2003) 7922–7930.
[80] R.S. Kang, C.M. Daniels, S.A. Francis, S.C. Shih, W.J. Salerno, L. Hicke, I. Radhakrishnan, Solution structure of a CUE-ubiquitin complex reveals a conserved mode of ubiquitin binding, Cell 113 (2003) 621–630.
[81] A.K. Sharma, G.P. Zhou, J. Kupferman, H.K. Surks, E.N. Christensen, J.J. Chou, M.E. Mendelsohn, A.C. Rigby, Probing the interaction between the coiled coil leucine zipper of cGMP-dependent protein kinase I alpha and the C terminus of the myosin binding subunit of the myosin light chain phosphatase, J. Biol. Chem. 283 (2008) 32860–32869.
[82] N. Gunasekara, B. Sykes, J. Hugh, Characterization of a novel weak interaction between MUC1 and Src-SH3 using nuclear magnetic resonance spectroscopy, Biochem. Biophys. Res. Commun. 421 (2012) 832–836.
[83] M.S. Titushin, Y.G. Feng, G.A. Stepanyuk, Y. Li, S.V. Markova, S. Golz, B.C. Wang, J. Lee, J.F. Wang, E.S. Vysotski, Z.J. Liu, NMR-derived Topology of a GFP-photoprotein Energy Transfer Complex, J. Biol. Chem. 285 (2010).
[84] M.J. Howard, H.J. Chauhan, G.J. Domingo, C. Fuller, R.N. Perham, Protein-protein interaction revealed by NMR T-2 relaxation experiments: the lipoyl domain and E1 component of the pyruvate dehydrogenase multienzyme complex of Bacillus stearothermophilus, J. Mol. Biol. 295 (2000) 1023–1037.
[85] A.D. Gossert, P. Bettendorff, C. Puorger, M. Vetsch, T. Herrmann, R. Glockshuber, K. Wuthrich, NMR structure of the Escherichia coli type 1 pilus subunit FimF and its interactions with other pilus subunits, J. Mol. Biol. 375 (2008) 752–763.
[86] K. Kami, R. Takeya, H. Sumimoto, D. Kohda, Diverse recognition of non-PxxP peptide ligands by the SH3 domains from p67(phox), Grb2 and Pex13p, EMBO J. 21 (2002) 4268–4276.
[87] W.P. Shao, S.C. Im, E.R.P. Zuiderweg, L. Waskell, Mapping the binding interface of the cytochrome b(5)-cytochrome c complex by nuclear magnetic resonance, Biochemistry 42 (2003) 14774–14784.
[88] S. Deep, S.C. Im, E.R.P. Zuiderweg, L. Waskell, Characterization and calculation of a cytochrome c(-)cytochrome b(5) complex using NMR data, Biochemistry 44 (2005) 10654–10668.
[89] T. Saitoh, T. Ikegami, M. Nakayama, K. Teshima, H. Akutsu, T. Hase, NMR study of the electron transfer complex of plant ferredoxin and sulfite reductase - Mapping the interaction sites of ferredoxin, J. Biol. Chem. 281 (2006) 10482–10488.
[90] K. Takeuchi, M. Yokogawa, T. Matsuda, M. Sugai, S. Kawano, T. Kohno, H. Nakamura, H. Takahashi, I. Shimada, Structural basis of the KcsA K+ channel and agitoxin2 pore-blocking toxin interaction by using the transferred cross-satu ration method, Structure 11 (2003) 1381–1392.
[91] M. Yokogawa, K. Takeuchi, I. Shimada, Bead-linked proteoliposomes: a reconstitution method for NMR analyses of membrane protein-ligand interactions, J. Am. Chem. Soc. 127 (2005) 12021–12027.
[92] K. Takeuchi, H. Takahashi, M. Sugai, H. Iwai, T. Kohno, K. Sekimizu, S. Natori, I. Shimada, Channel-forming membrane permeabilization by an antibacterial protein, sapecin - Determination of membrane-buried and oligomerization surfaces by NMR, J. Biol. Chem. 279 (2004) 4981–4987.
[93] O. Ichikawa, M. Osawa, N. Nishida, N. Goshima, N. Nomura, I. Shimada, Structural basis of the collagen-binding mode of discoidin domain receptor 2, EMBO J. 26 (2007) 4168–4176.
[94] D.M. Yu, A.N. Volkov, C. Tang, Characterizing dynamic protein-protein interactions using differentially scaled paramagnetic relaxation enhancement, J. Am. Chem. Soc. 131 (2009) 17291–17297.
[95] V.A. Villareal, T. Spirig, S.A. Robson, M. Liu, B. Lei, R.T. Clubb, Transient weak protein-protein complexes transfer heme across the cell wall of *Staphylococcus aureus*, J. Am. Chem. Soc. 133 (2011) 14176–14179.
[96] I. Diaz-Moreno, A. Diaz-Quintana, M.A. De la Rosa, M. Ubbink, Structure of the complex between plastocyanin and cytochrome f from the cyanobacterium Nostoc sp PCC 7119 as determined by paramagnetic NMR – the balance between electrostatic and hydrophobic interactions within the transient complex determines the relative orientation of the two proteins, J. Biol. Chem. 280 (2005) 18908–18915.
[97] M.D. Vlasie, R. Fernandez-Busnadiego, M. Prudencio, M. Ubbink, Conformation of pseudoazurin in the 152 kDa electron transfer complex with nitrite reductase determined by paramagnetic NMR, J. Mol. Biol. 375 (2008) 1405–1415.
[98] X. Xu, W. Reinle, F. Hannemann, P.V. Konarev, D.I. Svergun, R. Bernhardt, M. Ubbink, Dynamics in a pure encounter complex of two proteins studied by solution scattering and paramagnetic NMR spectroscopy, J. Am. Chem. Soc. 130 (2008) 6395–6403.
[99] A.N. Volkov, D. Ferrari, J.A.R. Worrall, A. Bonvin, M. Ubbink, The orientations of cytochrome c in the highly dynamic complex with cytochrome b(5) visualized by NMR and docking using HADDOCK, Protein Sci. 14 (2005) 799–811.
[100] J.-L. Berry, M. Phelan, R.F. Collins, T. Adomavicius, T. Tonjum, S.A. Frye, L. Bird, R. Owens, R.C. Ford, L.Y. Lian, J.P. Derrick, Structure and assembly of a trans-periplasmic channel for type IV Pili in *Neisseria meningitidis*, PLoS Pathog. 8 (9) (2012) e1002923.